Materials Transactions, Vol. 43, No. 11 (2002) pp. 2908 to 2912

EXPRESS REGULAR ARTICLE

Factors Affecting Bend Formability of Tempered Copper Alloy Sheets

Kouichi Hatakeyama[1], Akira Sugawara[2], Takuya Tojyo[3,*] and Keisuke Ikeda[3]

[1]*Manufacturing Division, DOWA Metal Co., LTD., Toyooka 438-0125, Japan*
[2]*Metallic Materials Laboratory, DOWA Mining Co., LTD., Toyooka 438-0125, Japan*
[3]*Depertment of Materials Processing, Graduate School of Engineering, Tohoku University, Sendai 980-8579, Japan*

Uniform deformation of tempered copper alloy sheets is small, and their bend formability depends largely on the amount of non-uniform deformation, which is complicatedly influenced by other factors in addition to the work-hardening exponent n. In this study, it has been shown that post-uniform elongation in the tensile test can be represented by two parameters, $(e_f - e_u)$ and f. The symbol e_f is the nominal strain at the breakage point, e_u the uniform elongation and f the parameter giving the degree of strain localization along the tensile axis. Good correlation between those parameters and bend formability was ascertained by experimental studies on C51900 and some other Cu alloy sheets. The experimental results showed that the introduced two parameters were not independent variables but mutually related. In addition, the nucleation and growth processes of surface wrinkles in bending, which finally led to cracking, were studied metallographically. A lot of micro necks first arose in the vicinity of grain boundaries, and part of them developed into the groove of wrinkles. Spacing between grooves appeared to correspond with the size and distribution of cube-oriented grains.

(Received August 2, 2002; Accepted September 20, 2002)

Keywords: *copper alloy sheet, uniform elongation, n value, post-uniform elongation, strain localization, bend formability*

1. Introduction

Copper alloy sheets are widely used in fabrication of electrical components for various electronic devices, because they have good spring performance and formability in addition to highly electrical conductivity. The miniaturization of electronic devices requires the development of high conductive materials with better formability and higher spring limits. It is commonly known that the work-hardening exponent n is a good measure of stretch and bend formability. Mild steel and aluminum alloy sheets used in the production of various construction components have relatively high n values of 0.2–0.25, because they are usually supplied in the fully annealed condition. However, Cu alloy sheets are formed after heat treatment at temperatures which are lower than those required for recrystallization, in order to keep higher strength and spring limits. Since the microstructure maintains the "as-rolled" state, the n value is about one-tenth or less than that of the fully recrystallized material. Nevertheless, some types of tempered Cu alloy sheets, especially Cu–Sn–P alloys (phosphor bronze), show a relatively large post-uniform elongation and present good bend formability. It is clear that the bend formability of tempered Cu alloy sheets depends mainly on the post-uniform elongation rather than uniform elongation.

A number of researchers have tried to analyze the factors affecting elongation in tensile deformation.[1–12] In 1965, Hsu *et al.*[1] reviewed the reports in this field, dating back to 1850. Later, Hart[7] introduced the strain-rate sensitivity m, as an important material factor affecting flow localization. The Hart's analysis provided a starting point for more precise formulation of uniform and post-uniform elongations. In 1984, Semiatin and Jonas[10] summarized the investigations on plastic instability and flow localization in detail. Moreover, the development of FEM has permitted to follow the necking growth analytically.[12] However, the understanding of post-uniform elongation is still insufficient. The reason why some tempered Cu alloy sheets with small n and m values result in large post-uniform elongation has remained unclear.

Post-uniform elongation directly reflects the development of flow localization, no matter what the controlling factors may be. If the degree of flow localization is evaluated quantitatively, it may become a good measure for the bend formability. In this study, we focussed on post-uniform elongation of the tempered Cu alloy sheets containing phosphor bronze, and formulated the strain distribution along the tensile axis with two materials parameters. And they were confirmed to correlate well with the bend formability. In addition, the development of wrinkles during bend deformation was studied metallographically. The occurrence of wrinkles finally leads to surface cracking. It is helpful in the improvement of the bend formability to reveal the growth mechanism of wrinkles.

2. Experimental Procedure

Sheets of H-tempered C51900 (Cu–6 mass%Sn–0.2 mass%P), 1/2H- and EHV-tempered C19025 (Cu–1.0 mass%Ni–0.9 mass%Sn–0.05 mass%P),[13,14] and H-tempered Cu–Ni–Si alloy (Cu–2.0 mass%Ni–0.5 mass%Si–0.5 mass%Sn–1.0 mass%Zn) were prepared for the present study. The sheet thickness was 0.2 mm except for Cu–Ni–Si alloys with a thickness of 0.25 mm. C19025 and Cu–Ni–Si alloys have roughly three times the electrical conductivity of C51900 and show great promise for fine pitch connectors.

The dimension of the tensile specimen is shown in Fig. 1. Tensile tests were conducted with a constant speed of 10 mm/min. In order to measure the strain distribution along the tensile axis, scales with a spacing of 2 mm, and 0.5 mm for materials in which the strain distribution curve changes sharply nearby the failure point, were marked on the specimen's surface. Moreover, the strain-rate sensitivity m was measured by changing the cross-head speed; 0.1–10–0.1 mm/min.

*Graduate Student, Tohoku University.

In bending deformation, the stress state on the outer surface varies in the range of uniaxial tension to plane-strain tension, depending on the ratio of the width (W) to the thickness (t) of the specimen.[15,16] Therefore, the bend tests were carried out with various W/t ratios and bending radii (R). The W-shape bending method with a bend angle of $\pi/2$ was used to simulate the practical forming of connectors. After the bend test, the outer surface and middle cross-section normal to the bend axis were observed using both laser and optical microscopes.

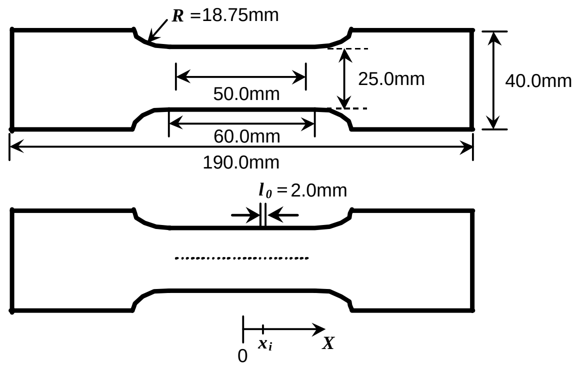

Fig. 1 Specimen for measuring strain distribution.

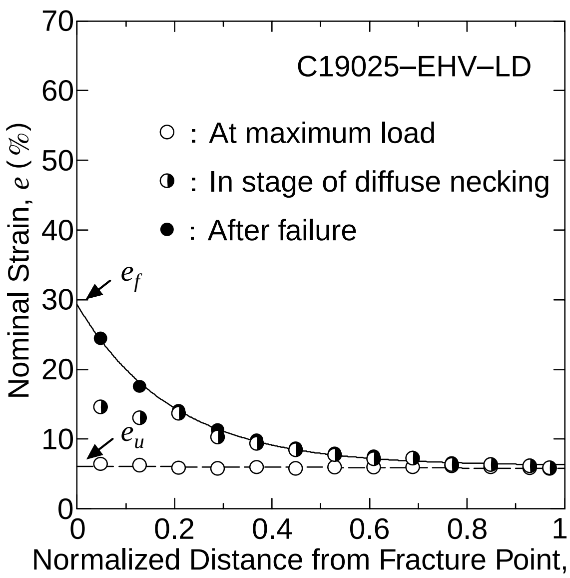

Fig. 2 An example showing development of strain distribution along the tensile axis.

3. Experimental Results and Discussion

3.1 Factors controlling uniform and post-uniform elongation

Figure 2 shows an example of the strain distribution in the tensile direction measured after tensile breakage. The sample is EHV-tempered C19025. As the figure, the experimental results fall on a curve given by the following empirical equation, which has been previously proposed by authors,[17,18)]

$$e(x) = e_u + (e_f - e_u) \times \exp(-x/f). \tag{1}$$

In the above equation, e_u is the uniform elongation, e_f the nominal strain at the breakage point, f the parameter representing the degree of strain localization and x the distance from the breakage point normalized by the gauge length. The unknown variables, e_f and f can be determined by the least square method.

The integration of eq. (1) gives the total elongation.

$$e_{total} = e_u + e_{pue} = e_u + (e_f - e_u) \times f \times \{1 - \exp(-1/f)\}. \tag{2}$$

As demonstrated in eq. (2), the post-uniform elongation is represented as a function of $(e_f - e_u)$ and f. It can be understood that the material with large $(e_f - e_u)$ and/or f values yields a large post-uniform elongation.

Table 1 illustrates the results of tensile tests, $(e_f - e_u)$ and f for all the tested materials. As the meaning of true stress and strain becomes lost due to neck growth, n values at the maximum load point, *i.e.*, the limits of the uniform strains are given in the Table 1. Only the LD sample of C51900 deformed uniformly with a constant load up to an elongation of 5.3% after the peak load. The n value at the start point of the tensile load drop is shown in parentheses.

Post-uniform elongation is mainly dependent on m, n and e_f. However, the strain-rate sensitivity m of all copper alloy sheets used in this study was less than 0.005 at room temperature. It has been confirmed by the FEM analysis that such a low value has only a negligible effect on the strain distribution. The n value obtained at the maximum load is nearly equal to the uniform true-strain $\ell n(1 + e_u)$, while no correlation between the post-uniform elongation and n can be seen, as shown in Table 1. The authors have found that the post-

Table 1 Mechanical properties of copper alloy sheets used in this research.

Alloy	Temper*	Tensile direction	Tensile strength σ_B (MPa)	n at load maximum	Uniform elongation e_u (%)	Post-Uniform elongation e_{pue} (%)	$e_f - e_u$ (%)	Strain distribution f
C51900	H	LD	629	0.0017 (0.052)	0.18 (5.3)	10.8	43.3	0.256
		TD	647	0.012	1.3	11.8	54.3	0.220
C19025	1/2H	LD	476	0.049	5.1	3.7	18.3	0.204
		TD	476	0.033	3.4	3.2	15.6	0.208
	EHV	LD	545	0.056	5.8	4.8	23.1	0.208
		TD	577	0.044	4.5	7.8	38.6	0.204
Cu–Ni–Si Alloy	H	LD	685	0.095	10.0	2.4	15.0	0.116
		TD	639	0.095	10.0	4.3	19.7	0.220

*1/2: Half Hard H: Hard EHV: Extra Hard (High Elongation)

Table 2 Width of hill and groove of wrinkles observed on bend surface.

Alloy		C51900				C19025								Cu–Ni–Si Alloy			
Temper		H				1/2H				EHV				H			
n		0.052		0.012		0.049		0.033		0.056		0.044		0.095		0.095	
$e_f - e_u$		43.3%		54.3%		18.3%		15.6%		23.1%		38.6%		15.0%		19.7%	
f		0.256		0.220		0.204		0.208		0.208		0.204		0.116		0.220	
W/t		LD		TD		LD		TD		LD		TD		LD		TD	
		2.5	50	2.5	50	2.5	50	2.5	50	2.5	50	2.5	50	2.0	40	2.0	40
$R/t = 0.5$	L_G (μm)	16.8	18.6	16.6	21.7	27.7	25.8	22.0	23.1	22.3	25.2	20.9	24.8	30.6	32.5	23.7	23.6
	W_b (μm)	5.9	5.8	6.1	6.7	9.9	9.1	5.6	10.2	5.2	8.4	4.3	15.9	9.2	11.5	4.6	11.5
	$W_{b(max)}$ (μm)	8.5	8.5	8.0	13.0	14.0	15.5	8.5	15.0	6.0	13.5	10.5	32.5	20.0	23.0	9.0	22.0
$R/t = 4.0$	L_M (μm)	10.4	9.8	10.2	11.2	11.7	12.4	11.8	12.3	11.8	11.5	13.5	12.5	10.7	11.6	10.9	15.0
	W_b (μm)	1.9	2.2	1.5	2.7	1.6	2.8	2.1	3.3	2.1	1.8	1.3	3.1	1.4	1.7	1.1	1.7
	$W_{b(max)}$ (μm)	3.5	4.0	2.5	5.0	2.5	8.5	3.5	7.5	3.5	3.0	2.5	7.0	2.5	3.0	1.5	3.5

uniform elongation is primarily influenced by the variation of n rather than its magnitude. Even if n at the maximum load point has a small value, an increase in n after the load peak delays necking growth. A typical example is tension in the transverse direction of the C51900 sheet. These details will be reported by the authors elsewhere. Considering the difficulty in accurately measuring the diverse variations of n in the necking stage, the proposed parameters, $(e_f - e_u)$ and f are more appropriate to represent quantitatively the degree of strain localization in tensile deformation.

3.2 Relationship between bend formability and proposed parameters

During the bending deformation, a number of micro necks were first observed on the outer surface. Then, part of them grew, resulting in surface wrinkles. The wrinkle grooves were made up of stepped new surfaces, while deformation on the hills of wrinkles was extremely minor. Photographs of the bent surface are shown in Fig. 3(a). The average width of micro necks and wrinkle grooves W_b (see Fig. 3(b)); the maximum width of micro necks and wrinkle grooves $W_{b(max)}$; the mean spacing between the micro necks L_M or between the grooves L_G, were measured using a laser microscope.

The results are summarized in Table 2. Increasing W/t from 2.5 to 50 (or from 2.0 to 40) raises W_b or $W_{b(max)}$. Simultaneously, L_G also increases, resulting in rougher surface wrinkles. In bending with $R/t = 4.0$, both L_M and W_b show insignificant differences among the tested materials. However, the H-tempered Cu–Ni–Si sheet having small $(e_f - e_u)$ and f presents large W_b, $W_{b(max)}$ and L_G in bending with $R/t = 0.5$, while the H tempered C51900 sheet having large $(e_f - e_u)$ and f small W_b, $W_{b(max)}$ and L_G. Clearly wrinkle development, which is a sign of surface cracking, depends on non-uniform deformation in tension and correlates not with n (or e_u) but with $(e_f - e_u)$ and f. And it can be understood from Table 2 that they are also good measures for formability in plane strain bending.

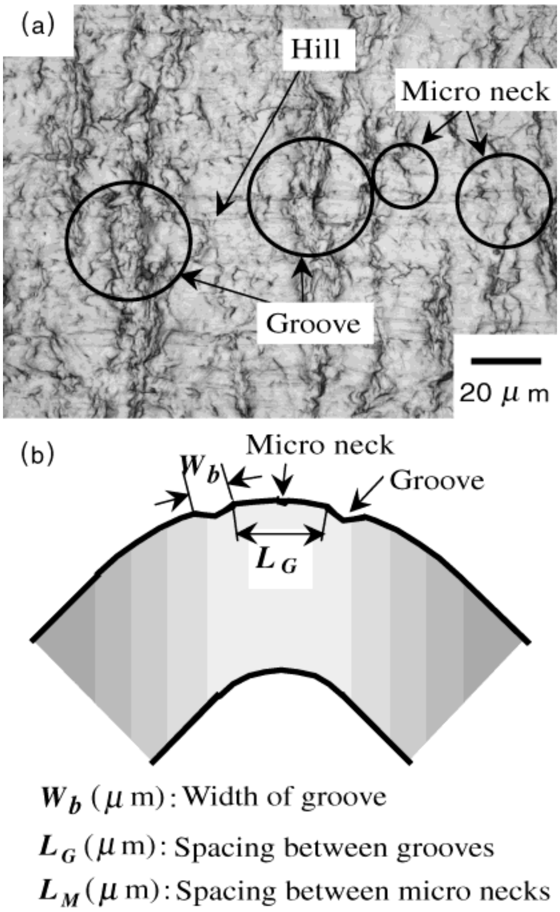

Fig. 3 The typical groove observed on bend surface.

3.3 Development of surface wrinkles in bending deformation

The formation and growth processes of surface wrinkles during bending were studied metallographically. The LD samples of H tempered C51900 and Cu–Ni–Si alloys were compared, because of a large difference in the n value, in spite of the similarities in total elongation. Additionally, there was a significant difference in the roughness of wrinkles.

The appearances of surfaces bent with $R/t = 4.0$ and 0.5 are shown in Figs. 4-a-1, b-1, a-2 and b-2, respectively, where e_{surf} represents the elongation on the outer surface. Figures 4-a-3 and b-3 show the optical microstructures before bending, in addition, Figs. 4-a-4 and b-4 show the distribution maps of cube-oriented grains obtained by EBSP.

The outer surface bent with $R/t = 4$ ($e_{\text{surf}} \fallingdotseq 11\%$) reveals an orange peel effect. This is verified by the value of L_{M} in Table 2 which shows that the periodical change in surface unevenness roughly corresponds to the size of the grain. The surface depression (micro neck) occurs in the neighborhood of grain boundaries, and high angle boundaries seem to bring about deeper micro necks. C51900 gives somewhat wider micro necks than Cu–Ni–Si alloy. At a surface elongation of less than 11%, noticeable micro necks have been observed on C51900 alone. A surface elongation of 11% is close to the uniform elongation of Cu–Ni–Si alloy and larger than that of C51900. These results suggest that formation of micro necks correlates with the n value.

In bending with $R/t = 0.5$ ($e_{\text{surf}} \fallingdotseq 50\%$), a remarkable development of wrinkles parallel to the bend axis is observed on both alloy sheets. However, the features of the wrinkles are different. Cu–Ni–Si alloy gives band-like wrinkle hills, while C51900 gives island-like ones. Such a difference is likely to result from the difference in the distribution of grain orientations.

Although the texture of C51900 was more similar to brass type while that of Cu–Ni–Si alloy to copper type, both alloys had similar textural components. A noticeable difference in texture was the higher intensity of the cube component in Cu–Ni–Si alloy. Distribution maps of cube-oriented grains are compared in a-4 and b-4 of Fig. 4. In Cu–Ni–Si alloys, relatively coarse grains of 10–15 µm in size are distributed with interspaces from 30 to 50 µm. Conversely, cube-oriented grains in C51900 are extremely fine and scattered uniformly with narrower interspaces from 10 to 20 µm. The cube component has large orientational differences compared to other components. Therefore, it is possible that the cube-oriented grains are connected to the development of micro necks into wrinkle grooves.

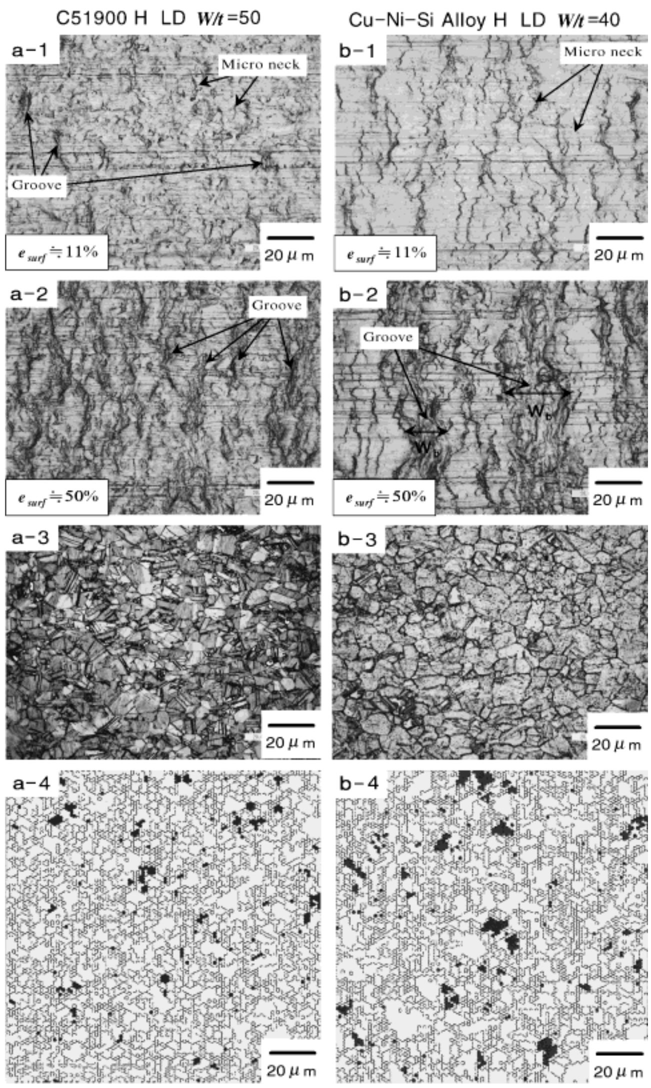

Fig. 4 Surface appearances after W-shape bending test carried out with $R/t = 4.0(1)$ and $0.5(2)$. Their initial micro structures(3). Their initial cube-oriented grains(4).

3.4 Estimation of ($e_{\text{f}} - e_{\text{u}}$) and f from uniform and total elongations

Although ($e_{\text{f}} - e_{\text{u}}$) and f have proven to be good measures for bend formability, it is laborious to determine them experimentally. A simple method for determining them is required.

Figure 5 is the diagram representing the relationship between e_{pue}, ($e_{\text{f}} - e_{\text{u}}$) and f. All of the experimental values are scattered around a solid curved line given by

$$e_{\text{pue}} = A \times (e_{\text{f}} - e_{\text{u}})^2 + B \times (e_{\text{f}} - e_{\text{u}}). \quad (3)$$

This fact means that ($e_{\text{f}} - e_{\text{u}}$) and f are not independent variables but mutually related. Accordingly, the bend formability of tempered Cu alloy sheets can be evaluated by either ($e_{\text{f}} - e_{\text{u}}$) or f. Considering that the variation width of ($e_{\text{f}} - e_{\text{u}}$) to a given increment of post-uniform elongation is larger than that of f, the former is a more appropriate measure for formability. Practically, ($e_{\text{f}} - e_{\text{u}}$) shows a better correlation with the post-uniform elongation than f, as seen in Table 1.

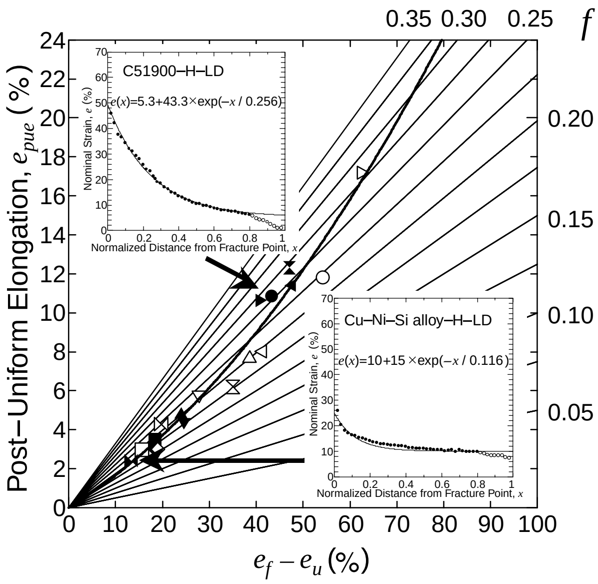

Fig. 5 Relationship between post-uniform elongation and ($e_{\text{f}} - e_{\text{u}}$).

Using the diagram presented in Fig. 5 helps to determine ($e_f - e_u$) or f by only uniform and total elongations in uniaxial tension. The strain-rate sensitivity of all materials used in this study has been small enough to negate its effect on necking growth. When the strain-rate sensitivity influences flow localization, the coefficients A and B in eq. (3) are supposed to vary significantly. It may be necessary to complete the diagram, taking the strain-rate sensitivity into consideration.

4. Conclusions

The formability of tempered Cu alloy sheets depends primarily on non-uniform elongation, because of low n values. In this study, the factors controlling the post-uniform elongation in tension have been researched, and a new measure for bend formability to take the place of n has been proposed. In addition, the development of surface wrinkles during bending, a sign of crack initiation, has been studied metallographically in detail.

The results are summarized as follows.

(1) The uniform elongation in uniaxial tension is given by the n value at the load peak, while the post-uniform elongation is represented as a function of ($e_f - e_u$) and f, where e_f is the nominal tensile strain at the breakage point, e_u the uniform elongation and f the parameter representing the degree of strain localization along the tensile axis.

(2) The roughness of surface wrinkles developed during bending has a positive correlation with ($e_f - e_u$) and f.

(3) The mean spacing between grooves of surface wrinkles corresponds approximately to the distribution width of the cube-oriented grains.

(4) Two parameters, ($e_f - e_u$) and f are not independent variables but mutually related. Accordingly, bend formability can be evaluated by either ($e_f - e_u$) or f.

(5) It has been shown that ($e_f - e_u$) and f can be simply determined from only uniform and total elongations in uniaxial tension.

REFERENCES

1) T. C. Hsu, G. S. Littleman and B. M. Marchbank: Proc. ASTM 65 (1965) 874–898.
2) G. E. Dieter: *Ductility*, (ASM, Metals Park, Ohio, 1968) pp. 1–30.
3) F. N. Mandigo and E. Shapiro: Metal Progress **108**-5 (1975) 101–102.
4) Y. Tomioka and J. Miyake: J. Japan Copper Brass Res. Assoc. **33** (1994) 232–236.
5) G. W. Stickley and D. J. Brownhill: Proc. ASTM **65** (1965) 597–616.
6) A. K. Ghosh: Metall. Trans. **5** (1974) 1607–1616.
7) E. W. Hart: Acta Metall. **15** (1967) 351–355.
8) D. A. Woodford: Trans. ASM **62** (1969) 291–293.
9) A. K. Ghosh: Trans. ASME **99** (1977) 264–274.
10) S. L. Semiation and J. J. Jonas: *Formability and Workability of Metals*, (ASM, Metals Park, Ohio, 1984) pp. 149–198.
11) D. K. Matlock and G. Krauss: *Formability and Metallurgical Structure*, (TMS-AIME, Warrendale, Pennsylvania, 1986) pp. 33–48.
12) K. Chung and R. H. Wagoner: Metall. Trans. A **19A** (1988) 293–300.
13) Akira Sugawara, Hiroto Narieda, Yoshitake Hana: IICIT Connector Symposium, Anaheim, California, (1999) 125–131.
14) L. Ling, A. Sugawara and K. Hatakeyama: J. Japan Copper Brass Res. Assoc. **40** (2001) 218–222.
15) E. L. Langer: *Bend Testing*, (ASM, Metals Park, Ohio, 1978) pp. 115–136.
16) J. H. Mendenhall: *Understanding Copper Alloys*, (John Wiley & Sons, New York, 1980) pp. 174–189.
17) K. Hatakeyama, Y. Hana, H. Narieda and A. Sugawara: Trans. JSSR. **44** (1999) 17–23.
18) K. Hatakeyama, A. Sugawara and K. Ikeda: J. Mater. Testing Res. Assoc. Japan **46** (2001) 226–233.